LA-UR- 95-3127

CONF-951222--1

Title: EXPERIMENTAL MEASUREMENT AND NUMERICAL SIMULATION OF RESIDUAL STRESSES IN A CARBURIZED LAYER OF A 5120 STEEL

Author(s): P. Rangaswamy, M. A. M. Bourke, J. C. Shipley, J. A. Goldstone

Submitted to: 1995 International Conference on Carburing and Nitriding with Atmospheres, Cleveland, OH, 6-8 Dec 95

1995 International Conference on Carburizing and Nitriding with Atmospheres, 6-8 December 1995; Cleveland Marriott Society Center; Cleveland, Ohio

Experimental measurement and Numerical simulation of residual stresses in a carburized layer of a 5120 steel

P. Rangaswamy, M.A.M. Bourke, J.C. Shipley & J.A. Goldstone

Los Alamos National Laboratory, Los Alamos, NM 87544

Abstract

A combined experimental and numerical study of residual stress and microstructure has been performed for a carburized steel 5120 specimen. Specimens were cut from 5120 steel bar stock, in the shape of hockey pucks and were subsequently carburized and quenched. X-ray diffraction was used to record stress profiles through the case for the martensite and retained austenite on the two flat surfaces oriented up and down during the quench. Layer removal was performed by electropolishing. Rietveld analysis was used to determine the lattice parameters of the phases at each depth varying with both carbon content and stress. The experimental measurements are compared with a numerical simulation of the phase transformation and the metallurgical changes following the carburization and quench. The results are discussed in the context of the microstructure and the role played by the retained austenite in interpretation. In addition the carbon profile obtained from the lattice parameters is compared with profiles measured using burnout.

CARBURIZING is a surface treatement process to ensure a certain residual stress state, hardness leading to improving wear and fatigue resistance. Carburization is qualitatively well understood and there are numerous publications elucidating this process [*].

One significant aspect of the carburizing process is the development of compressive residual stress which lends itself to beneficial properties. But, inevitably this also is accompanied by distortion of the parts. With a continuous increase in computing power and the steady decline of computational cost, there is currently much emphasis on modeling and simulation of commerical processes. As a result of this, even though the distortion and precursor residual stresses resulting from heat treatments have been widely studied, accurate predictions for new geometries remain elusive. Consequently, for the purpose of validating residual stress predictions, accurate measurements of residual stress and microstructure always remains a challenging enigma. The authors are not aware of any conclusive data which validate residual stress prediction by numerical tehniques.

The objective of this study is to compare experimental results with the results of numerical simulation. This is accomplished by performing a combined experimental and numerical study of residual stress in a carburized and quenched 5120 steel specimen in the shape of a hockey puck. In the experimental study, complementary depth profiles of residual stress and microstructure were recorded and analyzed through the carburized layer (containing a significant volume fraction of retained austenite) using conventional X-ray diffraction techniques and Rietveld method. X-ray diffraction technique was chosen because it is generally accepted as an Industry standard and has been extensively used for profiling residual stresses, by electropolishing, successive layers are removed exposing layers deeper into the material. Rietveld analysis was used to determine the lattice parameters of the phases (austenite & martensite) at each depth varying with both carbon content and stress. In addition to phase information, the use of Rietveld technique to calculate the changes in the lattice parameter provides an independent source for the carbon profiles, which is of extreme importance to the accurate prediction of distortion. Therefore by using Rietveld method in conjunction with the stress measurements, the carbon content can also be identified for relatively little extra effort. The experimental results are compared with a numerical simulation of the heat treatment of steel by quenching using TRAST a subroutine system used along with the finite element code ABAQUS. We have chosen the finite element program ABAQUS for our calculations since we are able to use the user subroutine UMAT (TRAST) which allows the modeling of the heat flux at the surface and metallurgical transformations. The numerical simulation is carried out in three steps; Carbon profile prediction using the mass diffusion material model provided in ABAQUS; the THERMAL/METALLUGICAL step using TRAST to calculate the temperature and phase compositions; & the MECHANICAL run from which the stresses and strains are calculated.

In the following sections, the Rietveld method and the finite element approach used is described briefly, relevant to purpose of the proposed study. A more complete description of both the techniques are available elsewhere (**).

Rietveld Technique.

The deduction of carbon from experimental powder diffraction data is made possible by the application of the Rietveld profile analysis technique. The philosophy of the Rietveld technique is that the entire diffraction pattern is treated as a single entity, so that peaks on the individual hkl reflections need not be resolved [*]. The method works by comparing the observed diffraction patterns to a calculated pattern from a hypothetical model; the parameters of the model are then refined to fit the observations. The refined variables include structural parameters (lattice constants, atomic positions and occupancies), peak shape parameters (strain and particle size), sample absorption, extinction and Debye-Waller factors. Some intstrumental parameters, including some of the diffractometer calibration constants, and a set of parameters for an emperical fit to the background, must also be fit. For a moderately complicated problem, the number of refined parameters might exceed 100, so that the routine application of the Rietveld method requires the use of powerful computers and reliable software.

The subroutine system TRAST [**]:

To model the simulation of carburization during quenching an user subrourtine system TRAST along with ABAQUS finite element code was used [*]. TRAST is capable of an accurate description of the material behavior of steel during quenching. Phase transformation are treated in detail including latent heat, volume change and transformation plasticity. Carburizing is treated by prescribing the carbon content as a field variable.

The computations are divided into two ABAQUS runs, and an interface program run. In the first run, the thermal condition, internal heat generation and the phase transformations are covered. In the second run, the mechanical behavior is treated, and the phase composition and temperature are considered as prescribed time dependent variable.

Even though TRAST, lends itself to be a powerful computation tool, it has certain limitations. The code does not incorporate the back coupling effect of the stress on phase transformations and temperature. Due to the difficulties in obtaining reliable data on the surface heat flux, the mechanical parameters of the different phases at elevated temperatures and most important, the transformation plasticity, predictions are in some cases inaccurate. The effects of tempering after the simulation of the carburized and quenching process is neglected. However, inspite of these limitations, still, TRAST is a very flexible and general research instrument, extremely suitable for these types of studies.

Materials and Experimental Procedure

Multiple cylindrical pucks (diameter 30 mm and thickness 10 mm were cut from 5120 bar stock having a composition detailed in table 1. One flat surface of each puck was polished and all the profiles were performed through this surface. The pucks were carburized for 35 hours at 1650 F at a carbon potential of 0.8, quenched and tempered.

TABLE 1

Composition of 5120 bar stock prior to carburization

Element	C	Mn	P	S	Si	Ni	Cr
Wt %	.23	.83	.012	.03	.22	.15	.8

Mo	Cu	Al	N	O
.04	.15	.031	.008	.003

Xray Diffraction Measurements.

Determination of near surface residual stress profiles is widely performed using X-ray diffraction and has been widely reported thus the details are discussed only as they are relevant to the neutron measurements [*]. In an XRD stress measurement using a soft wavelength typically the shallow region probed is assumed to be in a state of plane stress. This assumption forms the basis for the widely used d vs. $\sin^2\psi$ approach to calculating residual stress using equation 1.

$$\frac{d_{\phi\varphi} - d_0}{d_0} = \left(\frac{1+\nu}{E}\right)\sigma_\phi \sin^2\varphi - \frac{\nu}{E}\left(\sigma_{11} + \sigma_{22}\right) \qquad (1).$$

where $d_{\phi\psi}$ and d_o are the lattice spacing in the measured direction of the scattering vector and the unstressed lattice spacing respectively for any given set of hkl planes following the convention established by Dolle [*] ν and E are the poisson s ratio and elastic modulus respectively having values representative of the bulk material. $\frac{(1+\nu)}{E}$ and $\frac{\nu}{E}$ are the X-ray elastic constants. σ_ϕ is the direction of the stress measured on the sample surface.

Stress measurements were performed using standard methodology as outlined in SAE-J784A [*] with a Phillips vertical diffractometer operating at 40KV and 10mA. The spot was 2 mm in diameter. All measurements used Cr radiation (wavelength 2.289Å) for which the martensitic (211) reflection occurs at 156 (2θ) and the austenite (220) reflection at 128 (2θ). At the surface the martensitic reflection was 14 wide with 85% of the intensity coming from a width of 4 (2θ). At $\psi = 0°$ the penetration depth is 5.5 microns and at $\psi = 60°$ is 3 microns. A circular region 6 mm in diameter was electropolished at the center of the

puck using a mixture of phosphoric and sulfuric acids with distilled water (at 54 C), in the ratio of 2 : 1 : 1 by volume. The current was controlled at an approximate current density of 0.0042 A/mm^2 chosen to minimize surface pitting. Measured intensities were corrected for absorption at different ψ tilts, and normalized with respect to the Lorentz-Polarization factors. Background corrections were applied before calculating peak positions using the conventional parabolic technique.

Stresses in both martensite and austenite phases were calculated (using an x-ray elastic constant of 6.3 x 10^{-6} MPa^{-1}) in two orthogonal directions at the center of the puck. Both positive and negative ψ tilts were recorded (splitting was not observed). The raw stresses are shown in Figures 2 (a & b). Stresses were recorded to a maximum depth of 1.2 mm. Austenite volume fractions were also determined using the conventional technique comparing intensities of the austenite (220) and martensitic (200) reflections (Figure 3).

At each depth $\theta/2\theta$ scans from 40 to 162 2θ were recorded at $\psi = 0$ for Rietveld structure refinements using GSAS [13]. By assuming a body centered tetragonal structure (I4/mmm) for the martensite and, where appropriate close to the surface, a face centered cubic structure (Fm3m) for the retained austenite, predicted peak positions and intensities were matched to measured diffraction patterns. In addition to the lattice parameters, phase ratios, strain broadening terms were determined. Refinements for the surface and for a 1 mm depth are included in figures 4 (a,b). The tick marks indicate the positions of the peaks (including $K_{\alpha 1}$ and $K_{\alpha 2}$) and the difference between predicted and observed intensities is shown below. For the data at 1 mm depth, the austenite reflections are absent while the martensite reflections are sharper and displaced compared to the martensite reflections on the surface. From the Rietveld analysis of the data, both the lattice parameters of the austenite and martensite were recorded. It is well established that the c/a ratio of the martensite lattice parameter provides an independent measure of carbon [**] and this is shown in figure [**].

Numerical Simulation

A 2-D axisymmetric FEM mesh was used to model the carburized hockey puck, Figure **. At the very top part of the surface for about a 1mm in thickness, the mesh was finely graded in the form of layers of thickness 60 microns. This type of meshing was necessary to capture the stress and microstructure variation in the case of the carburized part. This type of meshing also allowed material removal simulation to simulate the effects of electropolishing to remove surface layers.

The material properties chosen are from a swedish steel which has similar composition, thermal and mechanical properties as the 5120 steel material used in the study. The heat transfer boundary conditions, extremely critical to model the heat flux at the boundaries, were treated as constant valued and applied at the boundaries (Top and Outside), in the ratio of 2:1. The values used were chosen out of experience and the actual values are being experimentally measured and will be used in the problem as and when they are available.

The first step in the numerical simulation is the calculation of the carbon profile. This is done separately using the mass diffusion material model available in ABAQUS. The carbon profile predictions from ABAQUS have been verified with predictions calculated using Marathon software and experimental results where available. As an example, one such set of results are shown in figure **, where the results of the FEM model and the Marathon model show excellent agreement.

The carbon profile is input as a field variable into the Trast-thermal/metallurgical run to calculate the microstructures as a result of phase transformation during the quenching of the carburized part. Figure ** show the fringe contours of the carbon profiles predicted after the completion of the carburizing cycle. The carbon varies from 0.8 wt-pct at the surface to 0.2 wt-pct at the interior for the carburizing cycle parameters used in the study.

Figure **, shows the fringe contours of austenite and martensite obtained after completion of the Trast-thermal/metallurgical run. The retained austenite decreases from a maximum of 25 % at the surface to a minimum of less than 2 % at about 600 microns depth. The martensite increases from a minimum of 75 % at the surface and reaches a threshold maximum of 99 % at about 600 microns depth. For the carburizing and quenching conditions used here, no other microstructures in the form of pearlite, bainite or ferrite was observed.

Figure **, shows the fringe contours of stresses (radial, hoop and axial, obtained after completion of the Trast-mechanical run. The radial and hoop stresses are compressive, with maximum compressive stress of about -420 MPa at the top and outside surface respectively, and, becoming tensile at about 1 mm in depth. The axial stress component is compressive on the outside surface, having approximately the same magnitude as the radial and hoop stresses, and tensile on the top surface having relatively small magnitudes of *** MPa.

Again, similar to the first author's work described in Ref **, carbon content, retained austenite and surface stresses were calculated by taking the average nodal (for carbon) and elemental (for austenite & stresses) quantities from each of the layers in the FEM mesh. Since, the spot size of 6 mm diameter was used for X-ray measurements, this corresponds to six elements in the radial direction from the axis of the FEM model. Subsequently, each surface layer corresponding

to six elements was "removed" and average stresses were computed for the next layer, to simulate the layer removal process. This procedure was used to determine the average stresses on the surface after the layer removal process.

Comparison of Experimental and Numerical simulation results.

Results of the numerical simulations are compared with experimental results in figures **, ** and ** for carbon, retained austenite and residual stresses respectively. In figure **, the carbon profile obtained from Abaqus FEM prediction is compared with the carbon profiles obtained from calculation using the c/a ratio of the martensitic lattice parameter and experimental measurements obtained through combustion techniques. Below 350 microns there is excellent agreement between the experimental measurements and FEM predictions, but closer to the surface the agreement is qualitative between the experimental measurements but clearly in dis-agreement with the FEM predictions. Further conclusions require metallography to establish whether only martensite and austenite are present - and further investigations into the modeling capability as to the possible ways de-carburizing effects could be accounted for.

In figure **, the retained austenite predictions using Trast is overlaid on the measurements using both conventional and Rietveld techniques. Even though the predictions and measurements show a fair agreement in the trends, it is clear that the predictions have underestimated the retained austenite content in the specimen. The measurements show, that the austenite varies from 20 vol% at the surface to a maximum of 30% at 50 microns, thereafter decreasing to less that 5% at about 600 microns depth. The predictions show a maximum austenite composition of 25 vol% at the surface and thereafter decreases to less than 4% at about the same depth as the measurements. An additional observation is that the lattice parameters as shown by the c/a ratio show a marked reduction in the first 100 microns. This appears to correlate with region of reduced austenite, and preliminary metallography suggests that this may be a decarburized layer.

In figure **, the predicted residual "radial"stresses are shown overlaid the corrected and un-corrected measured stresses. The corrected stresses are calculated using the Moore & Evan's technique which assumes a complete layer is removed in each step. The predicted stresses shown are for each of the layers before and after the layer removal process is completed. The layer removal process is simulated using the material change option in the Abaqus FEM code. Briefly, the material removal simulation is achieved within the FEM code by multiplying the stiffnesses by a severe reduction factor and running the analysis as a static analysis.

Here also, the comparison between the predictions and measurements is in fair agreement beyond 350 microns in depth. Over the first 200 microns from the surface, the measured stresses show considerable scatter but thereafter the profiles are smoother. For this type of heat treatment, the measurements indicate that the maximum compressive stress of -455 MPa is about 550 microns from the surface and rises quite sharply towards tensile stresses. If the measurements are compared with the layer removal predictions, there seems to be an excellent agreement between the predictions based on layer removal simulation and measured stress values. The Moore & Evans's correction to the measured stresses has an effect of decreasing the overall magnitude of the compressive stress, and increasing the tensile higher than the measured value. If the Moore & Evan's corrections to material removal process were to build up the original profile in the material before the layer removal, than the corrected stress seems to qualitatively agree with predictions in the layers before the layer removal process.

Summary & Conclusion

In this study we have demonstrated the effectiveness in combining an experimental and numerical study for a complex problem like this in understanding the development and measurement of residual stresses. We have been reasonably successful in comparing the predictions with the experimental results beyond the region effected by a possible "decarburized layer". The use of Rietveld method offers an independent method of indicative of decarburization as well as potentially offering a viable method for determining the carbon profile. The simulation of layer removal has been successfully accomplished by using the material change options available within the Abaqus FEM code.

1. Maximum compression is 600 microns below surface.
2. Using a Moore & Evans correction the crossover from compression to tension is between 1 and 1.2 mm below surface.
3. Austenite volume fraction ~ 25% at surface increasing slightly to a maximum of 30% at ~100 microns and subsequently falls to ~ 5% at a depth of 600 microns.
4. Martensite and austenite stresses in first 250 microns are not statistically different.
5. Maximum compressive stress corresponds to the position at which retained austenite volume fraction reaches a minimum of ~ 5% .

ACKNOWLEDGMENTS

This work was pursued as part of a DOE CRADA (#?) in collaboration with industry participants through the National Center for Manufacturing Sciences. We gratefully acknowledge Maurice Howes and Gerry Koller from IITRI for heat treating the specimens. We also acknowledge the use of Intense Pulsed Neutron Source operated as a national user facility by the United States Department of Energy, Basic

Engineering Sciences - Material Sciences, under contract No. W-31-109-ENG-38.

References:

1. Heat Treatment, Microstructures, and Residual Stresses in Carburized Steels, G. Krauss, Proceedings of the First Conference on Quenching & Control of Distortion, Chicago, Illinois, USA, 22-25 September 1992.
2. D. P. Koistinen, Trans. ASM, 1958, 50, 227.
3. Modeling Distortion and Residual Stress in Carburized Steels, M. Henriksen, D.B. Larson, and C. J. Van Tyne, Proceedings of the First Conference on Quenching & Control of Distortion, Chicago, Illinois, USA, 22-25 September 1992.
4. L. J. Ebert, Metallurgical Transactions A, Volume 9A, Nov 1978 (1537-1551)
5. R.C. Fischer, Metallurgical Transactions A, Volume 9A, Nov 1978 (1553-1560)
6. G. Krauss, Metallurgical Transactions A, Volume 9A, Nov 1978 (1527-1535)
7. R.B., Von Dreele, J.D. Jorgensen, & C.G.Windsor Journal of Applied Crystallography, 15, 581-589.1982
8. C. S. Robert, ∂Effect of Carbon on the Volume Fractions and Lattice parameters of Retained Austenite and Martensite, Trans. AIME, Journal of Metals, Feb, 1953, Pp 203-204.
9. Zenji Nishiyama, ∂Martensitic Transformation, 1978, Pp 14 - 20.
10. ∂Residual Stress Measurement by X-ray Diffraction, SAE Information Report J784a, M.E. Hilley, Ed., Society of Automotive Engineers, New York, August 1971.
11. Residual Stress, Measurement by Diffraction and Interpretation, I.C. Noyan and J. B. Cohen, Eds., Springer-Verlag, New York, (1987)
12. ∂Mathematical correction for stress in removed layers in X-ray diffraction residual stress analysis, M.G. Moore, W.P. Evans, SAE Transactions, p341 Vol66 1958.
13. A. C. Lawson and R. B. Von Dreele, Generalized crystal structural analysis system, LAUR 86-748, 1966 (Los Alamos National Laboratory)
14. B. Pardue and L. Lowery, ∂Four-Peak Retained Austenite Analysis using X-ray diffraction (XRD), Adv. X-ray Analysis, 43, (1994) - in publication.
15. Chongmin Kim, Adv. X-ray Analysis, 25, 1981, Pp 343-353.16. N. Jarvstrat: Two dimensional calculation of quench stresses in steel. Thesis no. 45, Linkoping Sweden, 1970.
17. HKS Inc.: ABAQUS User's Manual, Providence USA, 1993.
18. "Current Status of TRAST; a Material Model Subroutine system for the calculation of Quench stresses in steel. Niklaus Jarvstrat and Soren Sjostrom, Department of Mechanical Engineering, Linkoping University, S-581, 83 Linkoping, Sweden.

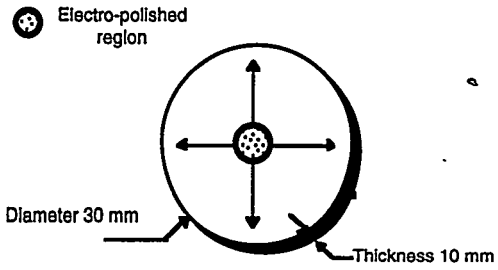

Figure 1. Schematic drawing of the Carburized Puck showing the measurement location and directions.

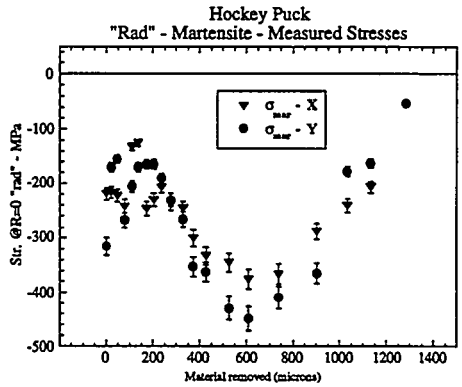

Figure 2 a. Residual stress profile in the martensitic phase (Un-corrected).

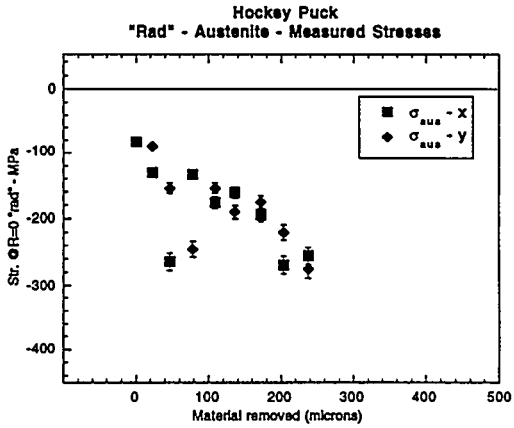

Figure 2 b. Residual stress profile in the austenite phase (Un-corrected)

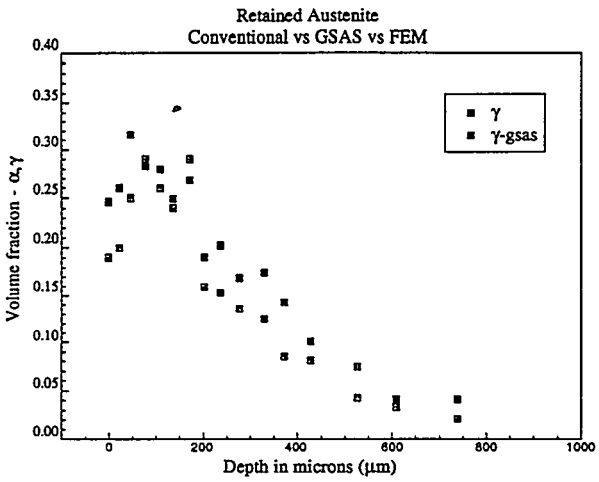

Figure **. Retained austenite profiles using both conventional x-ray techniques and Rietveld analysis of x-ray data.

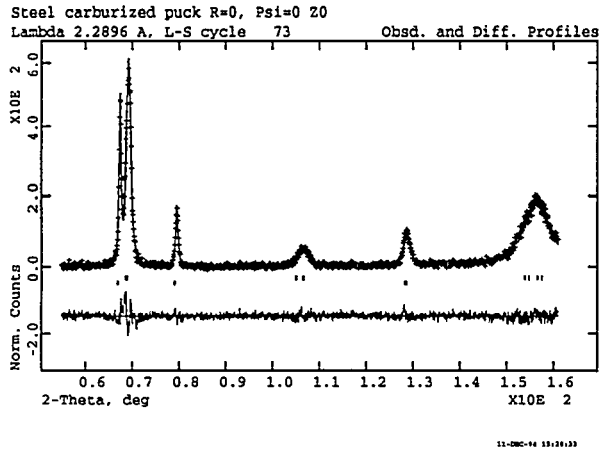

Figure **. Reitveld refinements for the surface showing both austenite and martensitic reflections.

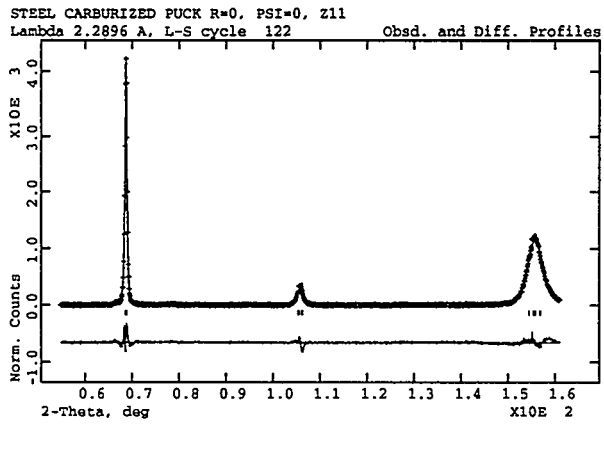

Figure **. Reitveld refinements at 1 mm depth below the surface showing martensitic reflections only.

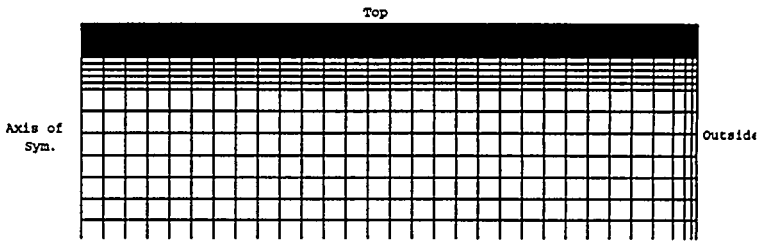

Figure **. A 2-D axisymmetric finite element mesh used to model the carburized hockey puck, showing the Top and Outside boundaries used for applying the boundary conditions

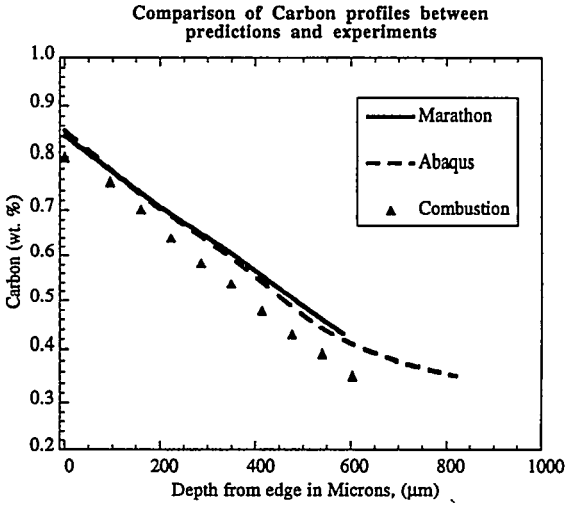

Figure **. Carbon profile predictions between experimental and predictions for a hypothetical test specimen.

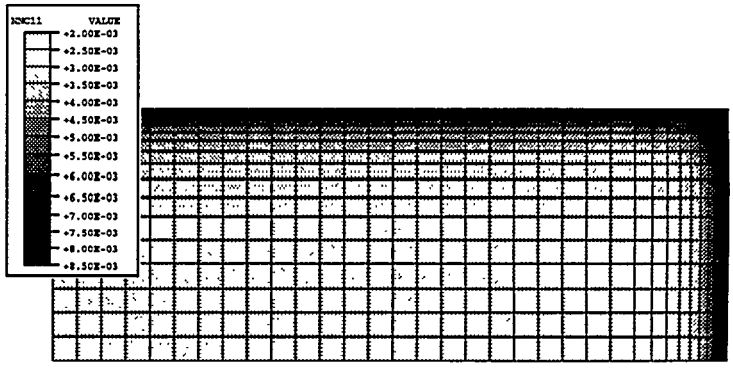

Figure **. Fringe contours of carbon variation in the carburized puck..

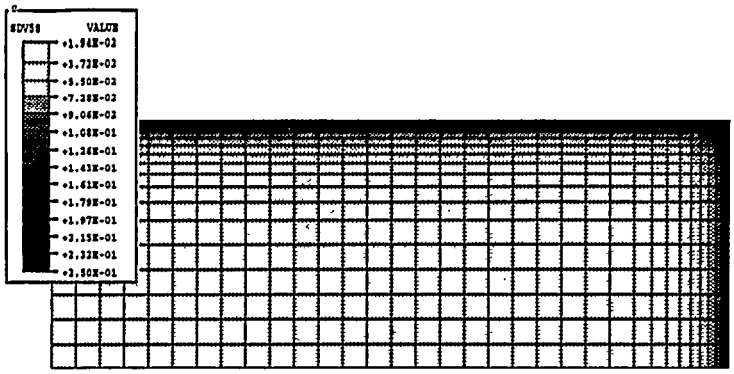

Figure **. Fringe contours of Retained Austenite variation in the carburized puck.

Figure **. Fringe contours of ɜAxial Stress in the carburized puck after the completion of the quenching process.

Figure **. Fringe contours of ɜRadial Stress in the carburized puck after the completion of the quenching process.

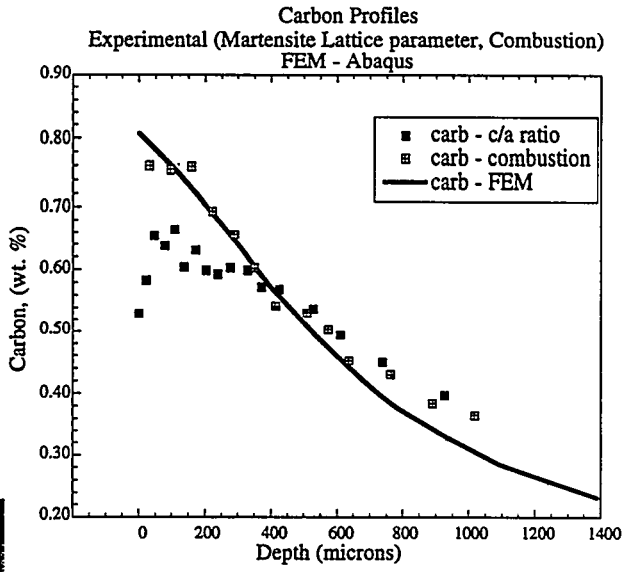

Figure **. Comparison of Carbon profiles between predictions from Abaqus, calculations from lattice parameters and experimental measurements using combustion (burn-up) technique.

Figure **. Fringe contours of ɜHoop Stress in the carburized puck after the completion of the quenching process.

DISCLAIMER

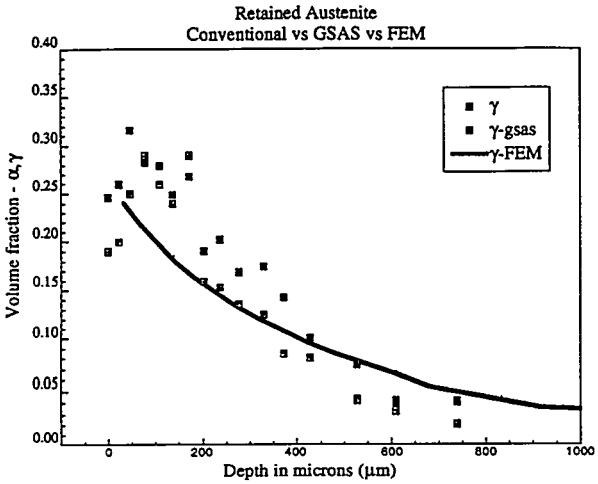

Figure **. Retained austenite profiles obtained from predictions based on TRAST and by measurements using both conventional x-ray techniques and Rietveld analysis of x-ray data.

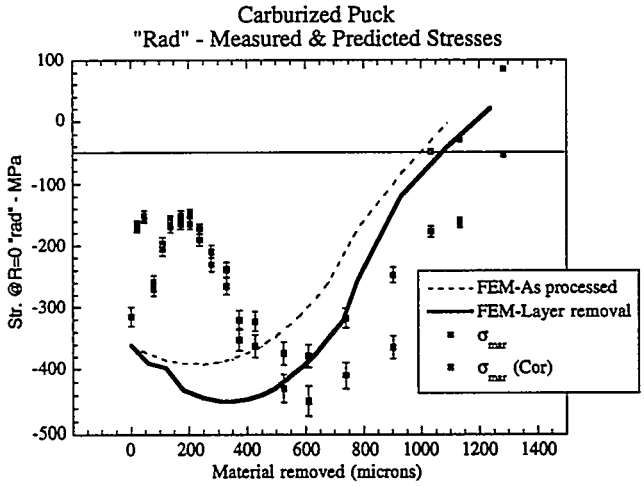

Figure **. Comparison of residual stress profiles between experimental measurements and TRAST predictions.